Publishing Excellence Inspiring Progress
ARISTON PUBLICATIONS
Quantum Advances
ISSN: 3143-0724 www.aristonpubs.com/journal/quantum-advances https://doi.org/10.69626/qa.2026.0105

RESEARCH ARTICLE

Approximating electron photon transition rates in quantum wells

Junior Tlotleng*, Perfect Jachi, Galebonwe Ramaphane, Godiraone Adelade Nkoni, Lefika Knight Maphage, Monkami Masale, Moletlanyi Tshipa

ABSTRACT: Transition rates of an electron confined in a quantum well due to interaction with photon (electromagnetic radiation) are approximated and compared with the exact results. The energy levels of the system were calculated using the Schrödinger equation within the effective mass approximation. Wave functions of an electron confined in a quantum well are approximated, which are in turn used to approximate optical transition rates when an electron interacts with electromagnetic radiation. The approximate wave functions exhibit close agreement with the exact functions at lower quantum states but become less accurate as the principal quantum number increases. The energy eigen values of the system increase with decreasing quantum well width and the accuracy of the approximate energy eigen values decreases for higher states. Transition rates are characterized by peaks which occur whenever the energy of the incident photon equals the energy difference between states. Since the accuracy of the approximations decreases for higher energy states, the positions of the peaks corresponding to transitions involving higher states become less accurate. Increase in temperature decreases peaks of absorption transition rates while it enhances peaks of emission transition rates, a behavior captured well by the approximations.

Keywords: Transition rates, Quantum wells, Approximate wave functions.

Received: 10 July 2026; Revised: 19 August 2026; Accepted: 05 September 2026; Published Online: 18 September 2026

1. INTRODUCTION

Quantum wells (QWs) are semiconductor structures with nanometer dimensions that confine charge carriers in a two-dimensional plane, resulting in quantization of energy levels in the direction of confinement. This confinement leads to unique electronic and optical properties that differ significantly from those of bulk materials. By manipulating the thickness of the wells, typically ranging from a few nanometers to tens of nanometers, energy spectra can be finely tuned, enabling a wide array of applications in optoelectronics [1] and quantum computing [2–4]. Quantum wells are fabricated typically employing advanced semiconductor growth techniques which include Molecular Beam Epitaxy (MBE) [5, 6], Chemical Vapor Deposition (CVD) [7, 8] and Hydride Vapor Phase Epitaxy (HVPE) [9, 10]. Quantum wells have revolutionized numerous technological sectors, for example optoelectronics [1], quantum computing [2] and sensors [11–13]. Due to the quantized energy levels, one of the interesting phenomena that occur in quantum systems is electronic transitions [14–16]. These transitions are central to various phenomena, including photoluminescence [17–19], absorption [20] and the functionality of optoelectronic devices [21–23]. In electron-photon interaction, energy conservation mandates that the energy of the incoming photon matches the transition energies, that is, the difference in energy of the two electronic states involved in the optical transition. Understanding these transitions paves the way for advancements in laser technologies and photonic applications [24, 25] and quantum computing [2, 26, 27], where control over electronic

Department of Physics, University of Botswana, Corner of Notwane and Mobuto Road, Private Bag 0022, Gaborone, Botswana

* Author to whom correspondence should be addressed: Tlotlengj@ub.ac.bw (J. Tlotleng)

© Ariston Publications 2026. All rights reserved.

states is crucial. Approximating complex results allows researchers and practitioners to focus on the most relevant phenomena, streamline their computational models, and reduce the dimensionality of their problem space. Approximations can provide insights into critical behaviors, facilitating timely decision-making in design and analysis. Moreover, by providing a practical balance between precision and performance, these approximations enable the iterative exploration of design spaces, ultimately advancing innovation in various fields. Thus, strategic use of approximations is essential in distilling complex results into meaningful insights, ensuring that valuable computational resources are effectively utilized while maintaining a focus on tangible outcomes. In our present work we approximate wave functions of an electron confined in a quantum well. We in turn use the wave functions to calculate energy levels and electronic optical transition rates in quantum wells due to electron-photon interactions. This research is organized as follows: the theoretical background is laid in Section 2, results and analysis are dealt with in Section 2.3 while the concluding remarks can be found in Section 3.

2. THEORY

The work presented here is concerned with interactions of electrons confined in a quantum well of width (L_x) with incident electromagnetic radiation. The focus of this research is on employing various approximate wavefunctions in order to obtain the optical transition rates between any relevant states. The Hamiltonian for the confined electron is given by

$$H = -\frac{\hbar^2\nabla^2}{2\mu} + V(x). \tag{1}$$

where μ is the effective mass of the electron, $\hbar = h/2\pi$ is the reduced Planck's constant, ∇ the del operator and $V(x)$ is confining electric potential, for this case given by

$$V = V(x) = \begin{cases} 0 & 0 < x < L_x \\ \infty & elsewhere. \end{cases}$$

The solutions of the Schrödinger equation for the system considered here are found to be

$$\begin{aligned} \psi_n(x,y,z) &= C_n\chi_n(x)Y(y)Z(z) \\ &= C_n \sin(\kappa_n x)e^{ik_y y}e^{ik_z z}. \end{aligned} \tag{2}$$

where C_n is the normalization constant, k_y and k_z are the wave numbers in the y and z directions and $\kappa = \sqrt{2\mu E_n/\hbar^2}$. The second boundary condition of continuity of the wave function at $x = L_x$ yields

$$\kappa L_x = n\pi, \tag{3}$$

where $n = 1, 2, 3, ...$ is an integer. The above condition (Eq. 3) can be used to obtain the confinement energies as

$$E_n = \frac{n^2\hbar^2\pi^2}{2\mu L_x^2}. \tag{4}$$

Thus, the total energy of an electron confined in a quantum well is

$$E_T = \frac{n^2\hbar^2\pi^2}{2\mu L_x^2} + \frac{\hbar^2 k_y^2}{2\mu} + \frac{\hbar^2 k_z^2}{2\mu}. \tag{5}$$

2.1 Approximate wave functions

Some few approximate x components of the wave function given in Eq. 2 for $n = 1 \rightarrow 6$ electron's states are herein listed:

$$\begin{aligned} &\chi_1(x) \sim (x - x^2) \\ &\chi_2(x) \sim (L/2 - x)(x - x^2) \\ &\chi_3(x) \sim (L/3 - x)(2L/3 - x)(x - x^2) \\ &\chi_4(x) \sim (L/4 - x)(L/2 - x)(3L/4 - x)(x - x^2) \\ &\chi_5(x) \sim (L/5 - x)(2L/5 - x)(3L/5 - x) \\ &\qquad\qquad (4L/5 - x)(x - x^2) \\ &\chi_6(x) \sim (L/6 - x)(L/3 - x)(L/2 - x) \\ &\qquad\qquad (2L/3 - x)(5L/6 - x)(x - x^2) \\ &.... \end{aligned} \tag{6}$$

The respective energies obtained from these approximate wave functions can be calculated via

$$E_n' = \int_0^{L_x} \psi_n'^*(x,y,z)\Big[-\frac{\hbar^2\nabla^2}{2\mu} + V\Big]\psi_n'(x,y,z) \tag{7}$$

where $\psi_n'(x,y,z)$ is the total normalized wave function with the x component approximated according to Eq. (6) and $\psi_n'^*(x,y,z)$ is the complex conjugate of the total wave function.

2.2 Optical transition rates

We consider plane polarized electromagnetic radiation

 © Ariston Publications 2026. All rights reserved.

incident on an electron confined in a QW. The electron in an initial state of energy E_i can absorb the energy of the EM radiation and transition to a final state of energy E_f, provided that the energy of the EM radiation equals the energy difference between the states, $\Delta E = E_f - E_i$. The rate at which this transition occurs can be calculated using the Fermi Golden rule [28]

$$W_{fi} = \frac{2\pi}{\hbar}|\langle\psi_f|H_{int}|\psi_i\rangle|^2\delta(E_f - E_i \pm \hbar\omega), \tag{8}$$

where the electron-photon interaction H_{int} is given by

$$H_{int} = -\frac{e}{\mu}\vec{A}_\omega\cdot\vec{p} = -\frac{e}{2\mu}A_0[e^{i(\vec{q}\cdot\vec{r}-\omega t)}+e^{-i(\vec{q}\cdot\vec{r}-\omega t)}]\hat{\epsilon}\cdot\vec{p} \tag{9}$$

Here, $\vec{q}$ is the photon field wave vector, $\vec{r}$ the electron position vector, $\hat{\epsilon}$ is the unitary polarization vector of the radiation field and A_0 is the amplitude of the vector potential. The amplitude of the vector potential can be written as $A_0 = \sqrt{(N_q\hbar)/(2\epsilon_0\epsilon_w\omega\Omega)}$, where N_q is the number of photons in volume Ω of the quantum well of dielectric constant ϵ_w and ϵ_0 is the permittivity of free space.

Now, for light linearly polarized in the x direction incident on the quantum well in the z direction, $\vec{q} = (0, 0, q_z)$ and $\hat{\varepsilon}\cdot\vec{r} = x$, thus, transition rates in a quantum well can be evaluated as

$$W_{fi} = \frac{n_{qA}e^2(E_f - E_i)^2L_x}{4\epsilon_0\epsilon_w\hbar^2\omega} \times \langle x\rangle^2\delta(E_f - E_i \pm \hbar\omega). \tag{10}$$

where n_{qA} is the number of photons in the quantum well with energy $\hbar\omega$ per unit transverse area ($A = L_yL_z$) and

$$\langle x\rangle = \int \psi'_n(x,y,z)x\exp(iq_zz)\psi_n(x,y,z)d\Omega = \frac{8\mu n'n[\exp(i(q_z - \Delta k_z)L_z) - 1]}{(q_z - \Delta k_z)L_z\pi^2(2n + \Delta n)^2(\Delta n)^2}, \tag{11}$$

for odd Δn, and vanishes for even Δn, where $\Delta n = n' - n$ and $\Delta k_z = k'_z - k_z$. This gives the selection rules for transitions in this system. In the above, $d\Omega = dxdydz$ being the elemental volume and the identity: $\vec{p} = [\mu(E_f - E_i)\vec{r}]/(i\hbar)$, in the Heisenberg equations of motion for operators [29], has been used to substitute out the momentum operator in Eq. (9). Thus, for an electron wave function of the form given in Eq. (2), absorption and the emission transition rates are found to be [30, 31], respectively,

$$W_{fi}^{abs} = W_0|\langle x\rangle|^2\delta(E_f - E_i - \hbar\omega) \tag{12}$$

and

$$W_{fi}^{em} = W_0|\langle x\rangle|^2\delta(E_f - E_i + \hbar\omega), \tag{13}$$

where $W_0 = n_{qA}e^2(E_f - E_i)^2L_x/(4\mu\epsilon_0\epsilon_w\hbar^2\omega)$. Finally, it is helpful especially for purposes of computation, to replace the Dirac delta function with a Lorentzian factor according to

$$\delta(E_f - E_i \pm \hbar\omega) \to \frac{\gamma}{\pi(E_f - E_i \pm \hbar\omega)^2 + \gamma^2},$$

in which γ is the linewidth of resonance. The total transition rate of the quantum system involves a summation of all the individual transition rates taking into account the transition probabilities of all the allowed transitions according to [32]

$$\Gamma_{fi}^{abs/em} = \sum W_{fi}^{abs/em}f_i(1 - f_f) \tag{14}$$

where f_i and f_f is the Fermi-Dirac distribution function for the initial and final state respectively.

3. RESULT AND DISCUSSION

This section is dedicated to the discussions of the results obtained from the previous section. In the computations here, the effective mass of an electron has been taken as $\mu = 0.067m_e$, m_e being the mass of a free electron, and linewidth of $\gamma = 4.74\ meV$. Comparisons of the $n = 1$ and $n = 2$ exact wave functions (Eq (2)) and approximate wave functions (Eq (6)) can be viewed in Figure 1. The approximate wave functions ($L_x = 100$ Å) are accurate for the ground state ($n = 1$), and become less so for the first excited state ($n = 2$). Although based on results not shown here, overall there is good agreement between the exact and approximate wave functions, nonetheless, there is loss of accuracy as n increases. This implies that the wave functions can be used to approximate quantum properties of states with low

© Ariston Publications 2026. All rights reserved.

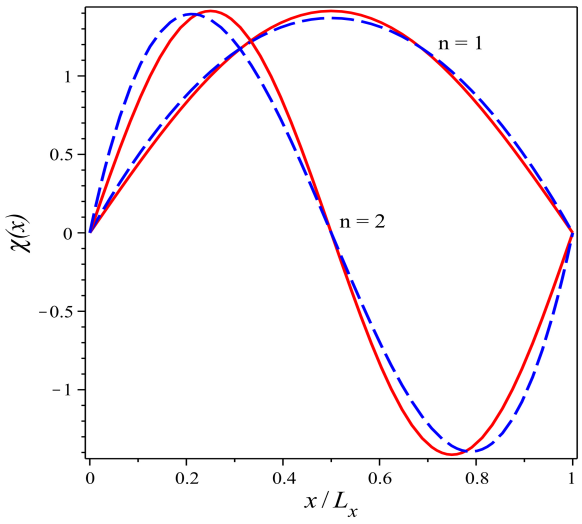

Fig. 1. Comparison of the exact wave functions (solid plots) and their approximations given in Eq (6) for the first two lowest lying states across a quantum well.

quantum numbers with reasonable accuracy. Both the exact and approximate solutions satisfy the boundary conditions $(\chi_1(x=0)=0)$ and $(\chi_1(x=L_x)=0)$, which is expected for a particle in an infinite quantum well.

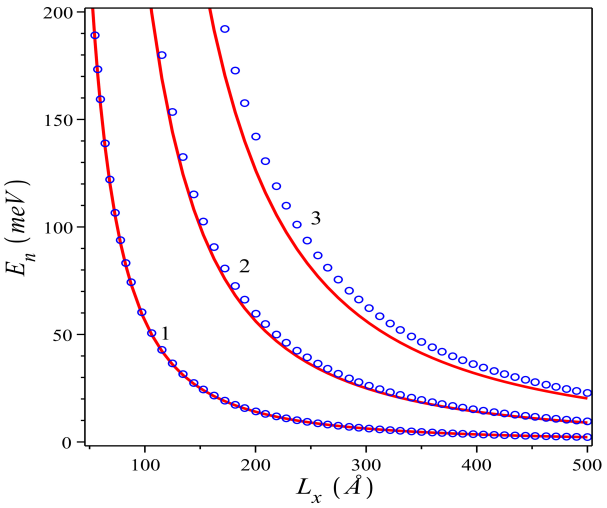

Fig. 2. Energy eigenvalues for an for an electron confined in a quantum well for the first three states. The solid plots are the exact values while the dashed plots with dots are the approximations obtained from Eq (7) from the wave functions given in Eq (6).

Figure 2 depicts the energy eigen values of an eigen values of an electron confined in a quantum well as functions of the quantum well width. The solid curves were obtained using the exact expressions, Eq (5), while the dashed plots with dots were obtained by utilizing the procedure outlined in Eq (7), using the approximate wave functions given in Eq. (6). The energy eigen values increase as width of the QW decreases, which is a result of increased confinement. States with higher n values have greater energy than those with lower values of n. It is seen in Figure 2, that there is good agreement between the exact and approximate energy eigenvalues, nonetheless and as anticipated, there is less accuracy with increasing principal quantum number n.

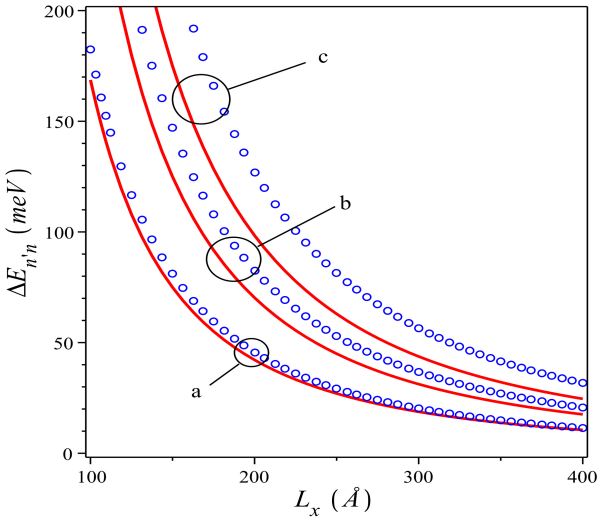

Fig. 3. Transition energies as functions of width of a QW, obtained from Eq (5) (solid plots) and those obtained Eq (7) (dashed curves) for the $\{n=1\rightarrow 2\}$ (a),$\{n=2\rightarrow 3\}$ (b) and the $\{n=3\rightarrow 4\}$ (c) transitions.

The dependence of transition energies on QW width can be viewed in Figure 3, which shows transition energies for the $\{n=1\rightarrow 2\}$ (a),$\{n=2\rightarrow 3\}$ (b) and the $\{n=3\rightarrow 4\}$ (c) transitions. The energy levels of electrons in a quantum well are quantized and depend on the width of the well. As the width of the well increases, the spatial confinement of the electron by walls of the potential well decreases and the energy levels converge. For narrow wells, the transition energies are higher due to stronger confinement, while for wider wells, the transition energies are lower as confinement is weaker. By adjusting the width of the quantum well, manufacturers can tailor the emission wavelengths of quantum well lasers and LEDs for specific applications and also optimize sensitivity to desired wavelengths hence improving the efficiency of, for example, photo-detectors. The approximate approach captures the general trend of how transition energies varies with the well width but is not as accurate as the exact approach,, particularly for excited states. This shows that the approximations are useful and can yield reasonable estimates for educational purposes or/and for initial designs of nanodevices, and beneficial when computational resources are limited.

 © Ariston Publications 2026. All rights reserved.

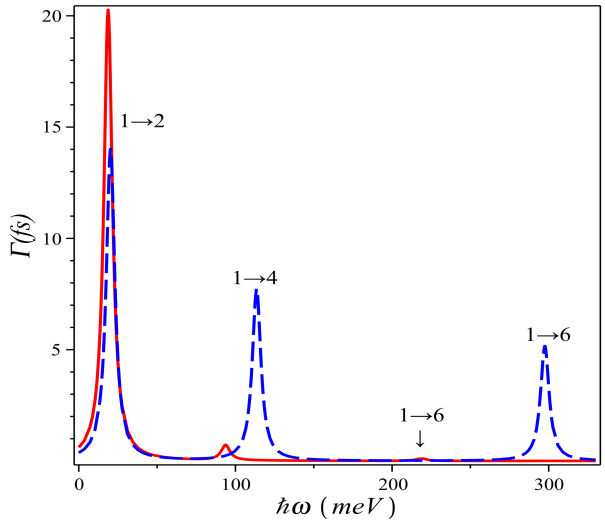

Fig. 4. Exact (solid plots) and approximate (dashed curves) absorption transition rates as functions of energy of the incident EM radiation for a QW of width $L_x = 200$ Å. The indicated peaks are for the $\{n = 1 \rightarrow 2\}$, $\{n = 1 \rightarrow 4\}$ and the $\{n = 1 \rightarrow 6\}$ transitions. The vertical arrow shows the position of the $\{n = 1 \rightarrow 6\}$ peak.

Figure 4 shows exact (solid plots) and approximate (dashed curves) the absorption transition rate as functions of energy of the incident EM radiation of a quantum well of width $L_x = 200$ Å with the indicated peaks for $\{n = 1 \rightarrow 2\}$, $\{n = 1 \rightarrow 4\}$ and the $\{n = 1 \rightarrow 6\}$ transitions and the vertical arrow indicates the position of the $\{n = 1 \rightarrow 6\}$ peak. The absorption transition rates depend significantly on energy of the incident EM radiation. When the incident photon energy matches the energy difference between two quantum states, the electron can absorb the photon and transition to a higher state. This results in peaks in the absorption spectrum at these resonant energies. The specific positions of these peaks depend on the quantum well's width and the energy level structure within the well. The exact method/ approach provides a more accurate and precise information about absorption peaks, essential for accurately predicting device behaviour and performance. They account for all interactions and effects within quantum well. Understanding absorption rates at specific energies allows for the design of devices like photo-detectors and solar cells, which maximize absorption at desired wavelengths, enhancing efficiency. In optical communication, optical components such as filters and modulators can be designed to operate efficiently at specific wavelengths used in communication. Although accurate, it requires comprehensive numerical solutions taking into account the full wave function and potential profile, which can be computationally demanding. As for the approximate method/approach, it offers a reasonable estimation of the absorption rates and peaks positions but may not capture all the finer details as peak magnitudes and slight shifts. This approximations are useful for initial designs and quick evaluations as it uses simplified approaches that reduce computational load where speed and resource efficiency is prioritized.

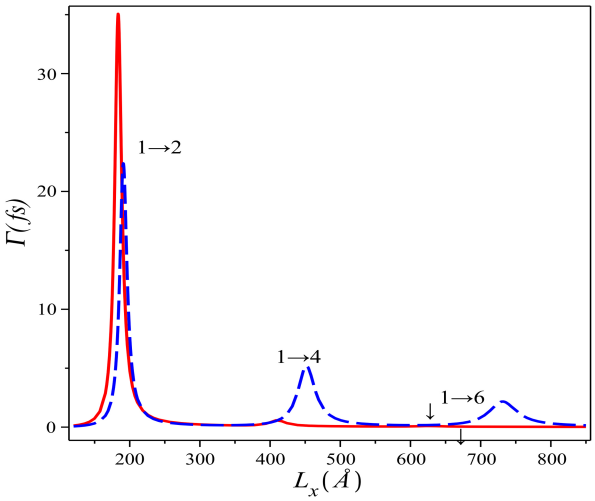

Fig. 5. Exact (solid plots) and approximate (dashed curves) absorption transition rates as functions of width of the QW for an EM radiation of energy $\hbar\omega = 50$ meV. The indicated peaks are for the $\{n = 1 \rightarrow 2\}$, $\{n = 1 \rightarrow 4\}$ and the $\{n = 1 \rightarrow 6\}$ transitions. The vertical arrow shows the position of the $\{n = 1 \rightarrow 6\}$ peak

Figure 5 shows exact (solid plots) and approximate (dashed curves) absorption transition rates as functions of width of the QW for an EM radiation of energy $\hbar\omega = 50$ meV. The indicated peaks are for the $\{n = 1 \rightarrow 2\}$, $\{n = 1 \rightarrow 4\}$ and the $\{n = 1 \rightarrow 6\}$ transitions. The vertical arrow shows the position of the $\{n = 1 \rightarrow 6\}$ peak. As already indicated, transitions from one state to the other are possible if the energy of the incident radiation (or any other source of energy) equals the difference in energy of the states between which a transition occurs. As such, transition rates are characterized by peaks whenever the energy of the radiation matches the transition energies. It is worth noting that transitions involving lower quantum numbers are more intense than those involving higher quantum numbers. This implies that the dominant transitions are those involving the ground state and other low-lying states. The approximated transition rates compared well with the exact transition rates, particularly for transitions involving low-lying states. The accuracy of the approximations diminishes with increasing value of n, both in magnitude and in the position of the peaks. As such, these approximations can be useful particularly for transitions involving low-lying states, which are the most intense and hence most

© Ariston Publications 2026. All rights reserved.

probable transitions in QWs.

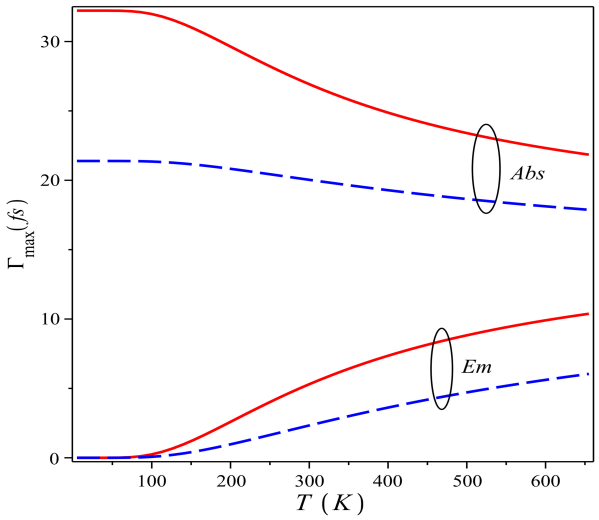

Fig. 6. The dependence of the exact (solid plots) and approximate (dashed curves) peaks of absorption (Abs) and emission (Em) $n = 1 \leftrightarrow 2$ transition rates on temperature for a QW of width $L_x = 200$ Å.

Figure 6 shows the temperature dependence of peaks of the $n = 1 \longleftrightarrow 2$ absorption and emission transition rates for a QW of width $L_x = 200$ Å, comparing exact results (solid lines) with approximate ones (dashed lines). The general pattern shows the peaks of absorption decreasing with increase in temperature while emission peaks increase with increasing temperature for both the exact and approximate approaches. However, the approximate method underestimates the absorption peaks for most of the temperature range and gets reasonably close only towards higher temperatures. As for the emission peaks, there is good agreement at lower temperatures, while at higher temperatures, the approximations underestimate the emission peaks.

4. CONCLUSION

In this study, electron-photon transition rates in quantum wells were approximated by utilizing approximate wave functions within the effective mass approximation. The approximate wave functions were used to estimate energy eigen values and optical transition rates, which were compared with the exact values. Our findings show that the results from the approximate wave functions concur with the exact values for lower quantum states but diverge as the principal quantum number increases. This pattern extends to energy eigenvalues and transition rates, where the approximations perform well for ground-state and low-lying states, but lose accuracy for higher states. We observed that the energy eigenvalues increase with decreasing quantum well width as a result of stronger confinement, a trend accurately captured by both exact and approximate methods for lower states. Furthermore, the transition rates exhibit characteristic peaks whenever the incident photon energy matches the energy difference between quantum states, with absorption peaks diminishing and emission peaks increasing as temperature rises. Although exact methods provide more precise results, approximations offer a practical alternative for initial designs and educational purposes, especially when computational resources are limited. These approximations can be useful in applications involving transitions between low-lying states, such as the design of optoelectronic devices like quantum well lasers and photodetectors. Although exact methods remain crucial for high-precision modeling, the approximations presented here offer a valuable tool for balancing accuracy and efficiency, advancing both fundamental research and technological innovation in semiconductor physics. Future work could focus on refining the approximations to extend their accuracy to higher states and exploring their implications in complex quantum systems. Furthermore, investigating the impact of external fields or material imperfections on these approximations could provide further insight into their practical applications.

DECLARATIONS

Ethical Approval

We affirm that this manuscript is an original work, has not been previously published, and is not currently under consideration for publication in any other journal or conference proceedings. All authors have reviewed and approved the manuscript, and the order of authorship has been mutually agreed upon.

Funding

Funding not available

Availability of data and material

The datasets used and/or analyzed during the current study are available from the corresponding author on reasonable request.

Authors' contributions

All the authors contributed substantially to the paper.

 © Ariston Publications 2026. All rights reserved.

Conflicts of Interest

The authors declare that they have no financial or personal interests that could have influenced the research and findings presented in this paper. The authors alone are responsible for the content and writing of this article.

REFERENCES

[1] Mu, Haoran and Yu, Wenzhi and Yuan, Jian and Lin, Shenghuang and Zhang, Guangyu, **2022**. Interface and surface engineering of black phosphorus: a review for optoelectronic and photonic applications. *Materials Futures*, 1(1), p.012301. https://doi.org/10.1088/2752-5724/ac49e3.

[2] Paquelet Wuetz, Brian and Degli Esposti, Davide and Zwerver, Anne-Marije J. and Amitonov, Sergey V., **2023**. Reducing charge noise in quantum dots by using thin silicon quantum wells. *Nature Communications*, 14(1), p.1385. https://doi.org/10.1038/s41467-023-36951-w.

[3] Sun, Y. and Xiao, J.-L., **2020**. Coherence effects of the strongly-coupled optical polaron-level qubit in a quantum well. *Superlattices and Microstructures*, 145, p.106617. https://doi.org/10.1016/j.spmi.2020.106617.

[4] Tshipa, Moletlanyi, **2023**. Probing semiconductor quantum well qubits and associated Shannon entropy. *Optical and Quantum Electronics*, 55(10), p.925. https://doi.org/10.1007/s11082-023-05043-w.

[5] Concordel, A. and Bleuse, J. and Jacopin, G. and Daudin, B., **2022**. The role of surface states and point defects on optical properties of InGaN/GaN. *Nanotechnology*, 34(3), p.035703. https://doi.org/10.1088/1361-6528/ac98cd.

[6] Shih, H.-J. and Lo, I. and Wang, Y.-C. and Tsai, C.-D. and Lin, Y.-C. and Lu, Y.-Y. and Huang, H.-C., **2022**. Growth and characterization of GaN/$In_xGa_{1-x}N$/$In_yAl_{1-y}N$ quantum wells by plasma-assisted molecular beam epitaxy. *Crystals*, 12(3), p.417. https://doi.org/10.3390/cryst12030417.

[7] Varshney, S. and Agarwal, Y. and Kalaichelvi, P., **2020**. A review of quantum dot solar cells fabrication via chemical vapor deposition method. In *AIP Conference Proceedings* (pp. 020002). https://doi.org/10.1063/5.0008169.

[8] Grützmacher, Concepcíon O. and Zhao, Q. T. and Buca, D., **2023**. SiGeSn alloys grown by chemical vapour deposition. *Applied Physics A*, 129, p.235. https://doi.org/10.1007/s00339-023-06478-4.

[9] Gil, E. and André, Y., **2021**. Growth of long III-As NWs by hydride vapor phase epitaxy. *Nanotechnology*, 32(16), p.162002. https://doi.org/10.1088/1361-6528/abdb14.

[10] Metaferia, W. and Braun, A. K. and Simon, J. and Packard, C. E. and Ptak, A. J. and Schulte, K. L., **2021**. Control of surface morphology during the growth of (110)-oriented GaAs. *Crystal Growth & Design*, 21(7), p.3916--3921. https://doi.org/10.1021/acs.cgd.1c00235.

[11] Yuan, J. and Gao, X. and Xie, M. and Shi, Z. and Cao, Z. and Wang, Y., **2024**. Optical proximity sensors using multiple quantum well didoes. *Optics Express*, 32(8), p.13955--13964. https://doi.org/10.1364/OE.522548.

[12] Chukeev, M. A. and Zheng, S. and Khramtsov, E. S. and Ignatiev, I. V. and Eliseev, S. A. and Lovtcius, V. A. and Efimov, M. A. Yu. P. and Lozhkin, S., **2024**. Excitonic sensor of electric field in quantum-well heterostructures. *Physical Review B*, 109, p.235305. https://doi.org/10.1103/PhysRevB.109.235305.

[13] Tan, C. L. and Mohseni, H., **2018**. Emerging technologies for high performance infrared detectors. *Nanophotonics*, 7(1), p.169--197. https://doi.org/10.1515/nanoph-2017-0061.

[14] Popov, V. N. and Henrard, L. and Lambin, P., **2005**. Electron-phonon and electron-photon interactions and resonant Raman scattering. *Physical Review B*, 72, p.035436. https://doi.org/10.1103/PhysRevB.72.035436.

[15] Fedorov, A. and Baranov, A. and Inoue, K., **1996**. Two-photon transitions in systems with semiconductor quantum dots. *Physical Review B*, 54(12), p.8627--8632. https://doi.org/10.1103/PhysRevB.54.8627.

[16] Pan, Y. and Cohen, E. and Karimi, E. and Gover, A. and Schönenberger, N. and Chlouba, T. and Wang, K. and Nehemia, S. and Hommelhoff, P. Kaminer, I., and Aharanov Y., **2023**. Weak measurements and quantum-to-classical transitions in free electron. *Light: Science & Applications*, 12(1), p.267. https://doi.org/10.1038/s41377-023-01292-2.

© Ariston Publications 2026. All rights reserved.

[17] Fang, Y. and Wang, L. and Sun, Q. and Lu, T. and Deng, Z. and Ma, Z. and Jiang, Y. and Jia, H. and Wang, W. and Zhou, J. and Chen, H., **2015**. Investigation of temperature-dependent photoluminescence in multi-quantum wells. *Scientific Reports*, 5, p.12718. https://doi.org/10.1038/srep12718.

[18] Guo, W. and Sun, H. and Torre, B. and Li, J. and Sheikhi, M. and Jiang, J. and Li, H. and Guo, S. and Li, K.-H. and Lin, R. and Giugni, A. and Fabrizio, E. D. and Li, X. and Ye, J., **2018**. Lateral-Polarity Structure of AlGaN Quantum Wells. *Advanced Functional Materials*, 28, p.1802395. https://doi.org/10.1002/adfm.201802395.

[19] Sun, H. and Mitra, S. and Subedi, R. C. and Zhang, Y. and Guo, W. and Ye, J. and Shakfa, M. K. and Ng, T. K. and Ooi, B. S. and Roqan, I. S. and Zhang, Z. and Dai, J. and Chen, C. and Long, S., **2019**. Unambiguously enhanced ultraviolet luminescence of AlGaN wavy quantum well. *Advanced Functional Materials*, p.1905445. https://doi.org/10.1002/adfm.201905445.

[20] Ciano, C. and Virgilio, M. and Montanari, M. and Persichetti, L. and Di Gaspare, L. and Ortolani, M. and Baldassarre, **2019**. Control of electron-state coupling in asymmetric Ge/Si-Ge quantum wells. *Physical Review Applied*, 11, p.014003. https://doi.org/10.1103/PhysRevApplied.11.014003.

[21] Shim, J. and Park, H.-Y. and Kang, J.-O. and Kim, D.-H. and Jo, S.-H. and Park, Y. and Park, J.-H., **2017**. Electronic and optoelectronic devices based on two-dimensional materials. *Advanced Electronic Materials*, 3(4), p.1600364. https://doi.org/10.1002/aelm.201600364.

[22] Wang, F. and Wang, Z. and Jiang, C. and Yin, L. and Cheng, R. and Zhan, X. and Xu, K. and Wang, F. and Zhang, Y. and He, J., **2017**. Progress on electronic and optoelectronic devices. *Small*, 13, p.1604298. https://doi.org/10.1002/smll.201604298.

[23] Cheng, J. and Wang, C. and Zou, X. and Liao, L., **2018**. Recent advances in optoelectronic devices based on 2D materials. *Advanced Optical Materials*, p.1800441. https://doi.org/10.1002/adom.201800441.

[24] Yang, Z. and Pelton, M. and Fedin, I. and Talapin, D. V. and Waks, E., **2017**. A room temperature continuous-wave nanolaser using colloidal quantum wells.. *Nature Communications*, 8, p.143. https://doi.org/10.1038/s41467-017-00198-z.

[25] Wu, J. and Chen, S. A. and Liu, H., **2015**. Quantum dot optoelectronic devices. *Journal of Physics D: Applied Physics*, 48(36), p.363001. https://doi.org/10.1088/0022-3727/48/36/363001.

[26] Ivády, V. and Davidsson, J. and Delegan, N. and Falk, A. L. and Klimov, P. V. and Whiteley, S. J. and Hruszkewycz, S. O. and Holt, M. V. and Heremans, J. and Son, N. T. and Abrikosov, I. A. and Gali, A., **2019**. Stabilization of point-defect spin qubits by quantum wells. *Nature Communications*, 10, p.5607. https://doi.org/10.1038/s41467-019-13495-6.

[27] Wang, C.-A. and Ercan, M. F. and Gyure, M. F. and Scappucci, G. and Veldhorst, M. and Rimbach-Russ, M., **2024**. Modeling of planar germanium hole qubits in electric and magnetic fields. *npj Quantum Information*, 10, p.102. https://doi.org/10.1038/s41534-024-00897-8.

[28] Rapp, C. S. and Franz, J. C. and Buhmann, S. Y. and Franca, O. J., **2025**. Purcell effect in chiral environments: A macroscopic QED perspective. *Physical Review A*, 112, p.013109. https://doi.org/10.1103/9k2w-rvcm.

[29] Scully, M. O. and Zubairy, M. S., **1997**. Quamtum Optics, Cambridge University Press, Cambridge. .

[30] Nag, B. R., **2000**. Physics of Quantum Well Devices, Kluwer Aca- demic Publishers, Dordrecht, Netherlands.. .

[31] Ridley, B. K., **1999**. Quantum Processes in Semiconductors. .

[32] Kumar, V. and Pratap, S. and Tshipa, M. and Masale, M., **2024**. Optical transition rates of a polar quantum disc with conical disclination in a magnetic field. *The European Physical Journal Plus*, 139(12), p.1--11. https://doi.org/10.1140/epjp/s13360-024-05909-2.

 © Ariston Publications 2026. All rights reserved.